INNSPUB

International Journal of Biosciences | IJB |
ISSN: 2220-6655 (Print) 2222-5234 (Online)
http://www.innspub.net
Vol. 13, No. 4, p. 378-386, 2018

RESEARCH PAPER OPEN ACCESS

Morphological and molecular analysis of commercial *Cordyceps militaris* strains in Thailand

Junya Nopparat[1], Kawee Sujipuli[1,5], Wassana Chatdumrong[*2,3,4]

[1]*Department of Agricultural Science, Faculty of Agriculture Natural Resources and Environment, Naresuan University, Phitsanulok, Thailand*

[2]*Department of Microbiology and Parasitology, Faculty of Medical Science, Naresuan University, Phitsanulok, Thailand*

[3]*Center of Excellence for Medical Biotechnology, Naresuan University, Phitsanulok, Thailand*

[4]*Centre of Excellence in Fungal Research, Naresuan University, Phitsanulok, Thailand*

[5]*Center for Agricultural Biotechnology, Naresuan University, Phitsanulok, Thailand*

Key words: *Cordyceps militaris*, Entomopathogenic fungus, Fungal morphological characteristic, Molecular marker.

http://dx.doi.org/10.12692/ijb/13.4.378-386 Article published on October 30, 2018

Abstract

Cordyceps militaris, an entomopathogenic fungusi, has been extensively utilized for many years as a functional food and for medicinal activities in Thailand. The fungus has numerous strains which are commonly sold in herbal markets and not all have been identified. Seven commercial *C. militaris* strains (CM-s1, CM-s2, CM-s3, CM-s4, CM-s5, CM-s6 and CM-s7) were studied using macroscopic methods (mycelium growth), microscopic methods (cross section and SEM techniques), and molecular markers. Most strains recorded high mycelial growth rates at colony diameters of 7.81±0.20 to 8.50±0.00cm after 18 days, with strain CM-s4 the lowest at 6.24±0.19cm. Characteristics of the stromal cross section in all strains observed under a microscope were golden yellow at the edge with colorless hyphae. A few conidia of all strains observed by SEM had oval shapes but most had globose shape with more single than short chain conidia. Genetic diversity among the seven strains gave 100% nucleotide-sequence homology at the ITS and 28S rRNA regions. These data suggested that the macroscopic method was a highly powerful tool for strain identification of *C. militaris*.

* **Corresponding Author:** Wassana Chatdumrong ✉ wassanac@nu.ac.th

Introduction

Cordyceps militaris is an entomopathogenic fungus whose spore invades and grows in a specific insect host as a caterpillar which hibernates underground during the winter season. Later, during the summer season, the spore develops into a fruiting-body formation on the surface of the insect's cadaver (Guo *et al.*, 2017). In Chinese traditional medicine, the fruiting body of *C. militaris* is credited with several pharmacological properties, and widely used as a herb, functional food, for improvement of immunity (Izgi *et al.*, 2015; Liu *et al.*, 2016; Song *et al.*, 2016), for bacteriostasis (Avtonomova *et al.*, 2016; Chiu *et al.*, 2016), antitumor (Zhang *et al.*, 2015), antiasthmatic effects (Tianzhu *et al.*, 2015), and as a antihyperuricemic (Yong *et al.*, 2016 and antihypoglycemic (Ma *et al.*, 2015).

Main abundant bioactive compounds produced by various *Cordyceps* species were adenosine (Tatani *et al.*, 2016), ergosterol, mannitol and exopolysaccharide (Raethong *et al.*, 2018), and cordycepin (Yong *et al.*, 2018) of these, cordycepin is an extremely valuable bioactive compound produced only by *C. militaris*. Artificial cultivation gives higher production of cordycepin compared to nature; however, its quality and quantity depend on fungal culture media (Lin *et al.*, 2018), culture conditions (Sung *et al.*, 2011), and strains (Wen *et al.*, 2017).

Recently, *C. militaris* has been isolated and estimated to many strains in Asian counties (Kang *et al.*, 2017) including in Thailand (Tanya, 2 0 1 2), where strains contained various amounts of cordycepin (Wen *et al.*, 2017). Therefore, classification among strains of *C. militaris* was beneficial to screen for strains that were able to produce high cordycepin content. During the past decade, two methods were widely used for morphological classification of *C. militaris* strains consisting of macroscopic such as mycelium growth (Dang *et al.*, 2017) and microscopic such as cross section (Guo *et al.*, 2017) and SEM techniques (Albini *et al.*, 2017). Recently, molecular genetic classification consisting of internal transcribed spacer (ITS) (Lam *et al.*, 2015) and 28S rRNA regions (Li *et al.*, 2013) has gained prominence.

Therefore, the aim of this study was to identify Thai commercial strains of *C. militaris* using both morphological characteristics and molecular genetic markers. Results will be beneficial by providing a rapid and accurate method for identification of commercial strains of Thai medicinal fungus *C. militaris*.

Materials and methods

Microscopic study of C. militaris through cross section of stroma

The fruiting bodies of *C. militaris* were collected from seven different commercial farms in Thailand (CM-s1, CM-s2, CM-s3, CM-s4, CM-s5, CM-s6 and CM-s7). The stroma was cut using cross section techniques and stained with lactophenol cotton blue. Morphological characteristics such as surface color, mycelium color and perithecium formation were observed under a microscope (Olympus CH30RF200, Japan) and photographed.

Macroscopic study of C. militaris through growth development

Individual fruiting bodies of *C. militaris* were collected from seven different commercial farms in Thailand. They were cut and plated on a potato dextrose agar (PDA) plate (containing 200g/l potato, 20g/l dextrose and 20g/l agar), and cultured at 25°C in the dark for 7 days. The end of each mycelium was cut and plated on a new PDA plate. Colony diameter (cm) was measured at 7, 14 and 21 days of culture. Mean comparisiond between *C. militaris* strains were calculated by were comparisons Duncan's Multiple Range Test (DMRT).

Microscopic study of C. militaris through SEM technique

Mycelium was individually cultured on PDA medium at 25°C under dark condition for 14 days. The growing mycelium was cut with sterile scalpels into small pieces (1x1cm) and fixed in 2.5% (v/v) glutaraldehyde. It was washed in 0.1M phosphate buffer for 15 minutes repeated twice and washed with 1% osmium tetroxide for 1 hour. The mycelium was then dehydrated through a series of 30, 50, 70, 90 and 100% ethyl alcohol for 30 minutes, respectively.

Finally, the mycelium was dehydrated in acetone for 30 minutes before mounting on an aluminum stub and coating with gold-palladium alloy. Spore structures were examined under a scanning electron microscope (LEO1455VP, United Kingdom(.

Genomic DNA (gDNA) extraction and PCR amplification

The medium, grown on PDA for 3-7 days, was collected for genomic DNA (gDNA) extraction using Insta Gene Matrix (Bio-Rad, United States) according to the manufacturer's instructions.

Two primer pairs as ITS primer pair (ITS1 and ITS4) and 28S rRNA primer pair (LR0R and LR7) were used in this study; their sequences are shown in Table 1. The primers of ITS1 and ITS4 were located on the 3´ end of 18S-rDNA border and the end of 28S rDNA border, respectively (Fig. 1). The ITS primer pair was used to amplify the DNA fragment to flank the entire ITS region and intervening 5.8S subunit (Fig. 1). The PCR reaction was carried out with 20 ng of gDNA as the template in a 30 µl reaction mixture using an EF-*Taq* (SolGent, Korea). The PCR condition was performed with the initial denaturation as follows: activation of *Taq* polymerase at 95°C for 2 minutes, followed by 35 cycles of 95°C for 1 minute, 55°C and 72°C for 1 minute each, and a final extension at 72°C for 10 minutes.

Meanwhile, the LR0R and LR7 primers were used for the DNA fragment at the partial 28S rRNA region. The amplified products were purified using a multiscreen filter plate (Millipore Corp., Bedford, MA, United States). Purified DNA samples were performed using a PRISM BigDye Terminator v3.1 Cycle Sequencing Kit (Applied Biosystems, Foster City, Canada) containing the extension products added to Hi-Di formamide. The mixture was incubated at 95°C for 5 minutes, followed by 5 minutes on ice, and then sequenced and analyzed using an ABI Prism 3730XL DNA analyzer (Applied Biosystems, Foster City, Canada).

DNA sequence alignment

Partial nucleotide-sequence reads were approximately 548 and 1223 nucleotides, amplified by ITS and 28S rRNA primer pairs, respectively. Both sequence reads were assembled using Bioedit Analysis software (Ta, 1999) and compared to known sequences of ITS and 28S rRNA regions of fungi published from the NCBI database using CLUSTAL W (European Bioinformatics Institute (EMBL-EBI), United Kingdom).

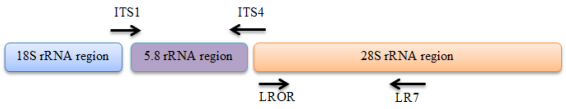

Fig. 1. Map positions of primer pairs (ITS1-ITS4 and LROR-LR7) used to amplify PCR. products.
Note: Primer ITS 1 is close to the 18S-rDNA border, and primer ITS 4 (5'-TCC TCC GCT TAT TGA TAT GC-3') anneals to 28S rRNA near the ITS 4 border.

Table 1. Primers used to amplify fungal ribosomal RNA genes and ITS region sequences.

Primer	Sequence (5'→3')	Reference
28S rRNA region		
LROR	ACCCGCTGAACTTAAGC	Bunyard *et al.* (1994)
LR7	TACTACCACCAAGATCT	Bunyard *et al.* (1994)
ITS region		
ITS1	TCCGTAGGTGAACCTGCGG	White *et al.*, (1990)
ITS4	TCCTCCGCTTATTGATATGC	White *et al.*, (1990)

Results and discussion

Mycelial growth and pigmentation characteristics

To assess growth and pigmentation characteristics of *C. militaris*, seven strains were cultured in potato dextrose agar (PDA) at 25°C in dark condition for 18 days, with data recorded every six days. Results revealed that mycelial growth and pigmentation characteristics were divided into three groups. Firstly, CM-s3 showed the highest growth rate followed by CM-s6, CM-s7, CM-s1 and CM-s5 with colony diameters ranging from 7.81±0.20 to 8.50±0.00cm after 18 days (Table 2). Mycelia showed abundant density and formed yellowish or yellow layers on PDA medium (Fig.2 and Table 3). Secondly, CM-s2 showed moderate growth rate, with colony diameter ranging from 7.05±0.40cm (Table 2) and the mycelia were formed as dense layers with rough and semi-cottony mycelial texture and yellow colony pigmentation (Fig.2 and Table 3).

Thirdly, CM-s4 had the lowest growth rate, with colony diameter ranging from 6.24±0.19cm (Table 2). Their mycelia were formed of dense layers with rough and semi-cottony texture and mustard yellow colony pigmentation (Fig.2 and Table 3). These results indicated that mycelial growth rates and characteristics were significantly different for each of the studied strains. This diversity might be caused by different culture periods and genotypes. Previous publications reported that mycelial growth rates and characteristics of *C. militaris* were significantly different depending on culture periods (Shrestha *et al.*, 2006), and genotypes (Lee *et al.*, 2013).

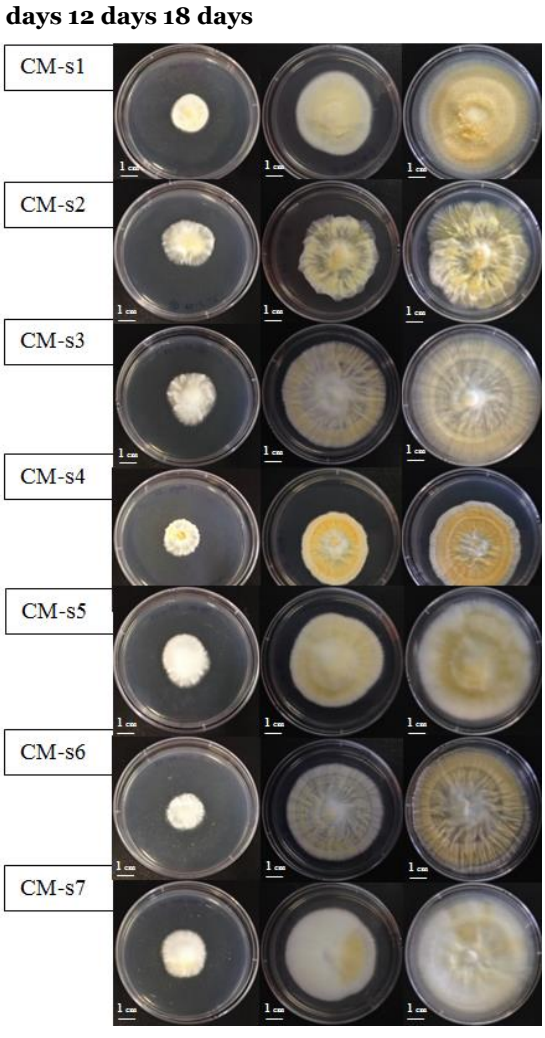

Fig. 2. Mycelial growth and characteristics among seven *C. militaris* strains)CM-s1 to CM-s7(cultured on PDA medium for 6, 12, and 18 days.

Microscopic characteristics of a stroma

Cross sections of individual stroma morphologies of the seven *C. militaris* strains were examined by staining with lactophenol cotton blue. All strains showed similar stromal characteristics with smooth yellow gold color outer cortex surfaces, and inner cortexes containing colorless hyphae without a perithecium (Fig. 3). These results indicated that the presence or absence of perithecia might be beneficially used to evaluate the morphological diversity of *C. militaris*. As supported by previous publications, some *C. militaris* species showed the presence of perithecia (Sung *et al.*, 2010) but other species did not have perithecia (Liu *et al.*, 2011) in the cortex region of the stroma.

In contrast, all *C. militaris* species had a smooth outer cortex surface and colorless hyphae at the inner cortex (Liu *et al.*, 2011).

Table 2. Colony diameter of seven *C. militaris* strains (CM-s1 to CM-s7) at different time periods cultured on PDA medium.

Strain	Colony diameter (cm) of *C. militaris*		
	6 days	12 days	18 days
CM-s1	2.83±0.06^{c}	6.06±0.14^{abc}	8.26±0.17^{ab}
CM-s2	3.25±0.08^{a}	5.48±0.24^{c}	7.05±0.40^{c}
CM-s3	3.31±0.04^{a}	6.45±0.22^{a}	8.50±0.00^{a}
CM-s4	2.50±0.17^{c}	4.46±0.31^{d}	6.24±0.19^{d}
CM-s5	3.08±0.21^{ab}	5.70±0.20^{bc}	7.81±0.20^{b}
CM-s6	2.78±0.21^{bc}	6.26±0.10^{ab}	8.45±0.05^{ab}
CM-s7	3.18±0.01^{ab}	6.70±0.15^{a}	8.43±0.06^{ab}

Note: colony diameter (cm) represented by mean ± SE was measured for all *C. militaris* strains. The same letters in each column indicate non-significant difference of mean values, calculated by DMRT at p-value ≤ 0.05.

Observation of conidial formation by Scanning Electron Microscopy (SEM)

Morphologies of the ascospores of seven *C. militaris* strains (CM-s1 to CM-s7) were determined using SEM. Results showed that most ascospores were globose and oval shaped which germinated to produce long hyphae. Most conidia were formed at the end of the hyphae as single globe heads but rare groups were globose in short chains. A few conidia formed as oval shapes (Fig. 4).

Table 3. Colony pigmentation of *C. militaris* (CM-s1 to CM-s7) on PDA medium.

Strain	Colony pigmentation					
	6 days		12 days		18 days	
	Margin	Center	Margin	Center	Margin	Center
CM-s1	Y	YW	W	YW to Y	W	Y
CM-s2	W to PY	YW	W to YW	Y	W to YW	Y
CM-s3	W to PY	PY	W to YW	W to PY	W to YW	W to YW
CM-s4	W to YW	MY	W to MY	MY	W	W to MY
CM-s5	W	W	W to YW	YW	W	W to Y
CM-s6	W	W	W to YW	YW	W to YW	W to YW
CM-s7	W to PY	W	W to Y	W	W to YW	W to YW

Note: W indicates white; Y indicates yellow; YW indicates yellowish white; PY indicates pale yellow; and MY indicates mustard yellow.

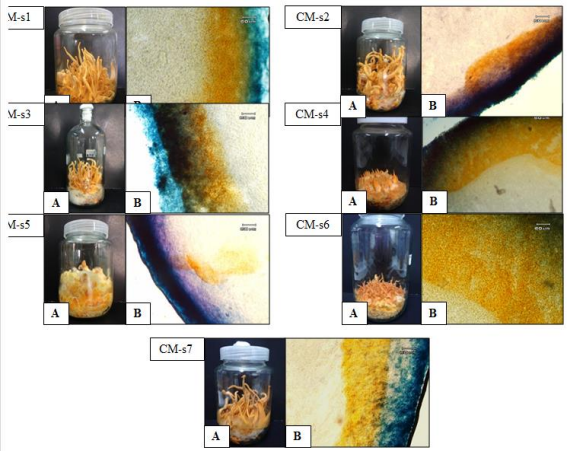

Fig. 3. Evaluation of stromal characteristics among seven *C. militaris* strains (CM-s1 to CM-s7) by cross section technique under a compound microscope.
Note: random stroma (A) were cross sectioned to examine microscopic characteristics (B); the scale bar indicates 10X (=60 µm).

As previously reported, hyphae of *C. militaris* (EFCC 11255) produce various forms of conidia, either as a single globose head or groups of globose short chains (Shrestha *et al.*, 2005). Moreover, conidia of *C. militaris* were presented as various shapes including globose (Tulasne and Tulasne, 1865) cylindrical and spherical)De, 1897 and Brown and Smith, 1957), almost spherical (Pettit, 1895), and oval (Petch, 1936). Seven commercial strains of *C. militaris* (CM-s1, CM-s2, CM-s3, CM-s4, CM-s5, CM-s6 and CM-s7) collected in Thailand were evaluated for morphological diversity using various macroscopic and microscopic methods. For the macroscopic studies, results concluded that most strains (except CM-s4) had high mycelial growth rate and abundant mycelial density, with rough and semi-cottony mycelial texture and yellowish colony.

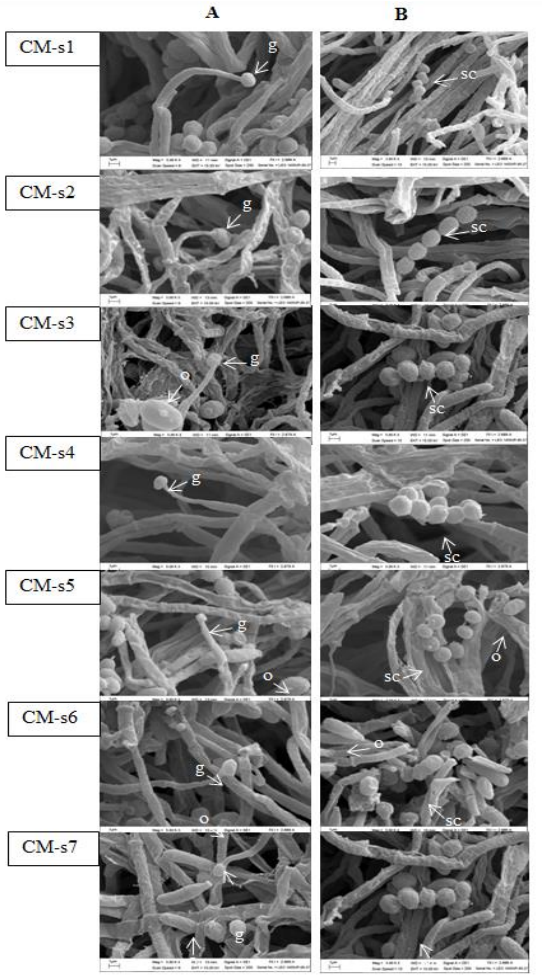

Fig. 4. Observation of conidial formation of *C. militaris* (CM-s1 to CM-s7) under a scanning electron microscope after culture on PDA medium for 14 days.
Note: conidial formations were either a single (A) or a group of short chains (B); g and o indicate globose and oval shape respectively; sc indicates short chain; and the scale bar indicates 1 µm.

Strain CM-s4 recorded the lowest growth rate and its mycelium was compact, formed of layers, and mustard yellow on PDA. For microscopic studies using a cross section technique, stromal characteristics revealed all strains as golden yellow at the edge with colorless hyphae. The conidial formation, investigated by SEM techniques, showed that most conidia were globose but a few had oval shapes. The globose conidial shape was mostly single with a few short chains. Commercial strains of *C. militaris* showed similar morphological characteristics which were not suitable for use in identification. Molecular genetics techniques were useful for further identification of *C. militaris* strains.

DNA sequencing analysis

Both the internal transcribed spacer (ITS) and 28S rRNA regions are highly divergent in nucleotide sequences and play a vital role in evolution among fungal species (Lam *et al.*, 2015). Therefore these areas were used to assess genetic diversity among the seven strains of *C. militaris* based on PCR assay. Two ITS primer pairs (ITS1 and ITS4) were used to amplify the DNA fragment flanking the entire ITS region and intervening 5.8S subunit, giving an ITS-PCR-fragment (548 bp long). Meanwhile, two 28S rRNA primer pairs (LROR and LR7) were used to amplify the DNA fragment at the 28S rRNA region, giving a 28S rRNA-PCR-fragment (1223 bp long). Nucleotide sequence reads of both the ITS-PCR-fragment and the 28S rRNA-PCR-fragment from individual strains were aligned using the ClustalW program and then compared to their known fungal sequences published from the NCBI database. Nucleotide sequences from all the studied strains gave 100% similarity, indicating that the seven strains of *C. militaris* did not have genetic distance at the ITS and 28S rRNA regions. These distance values of the ITS and 28S rRNA regions among the seven strains were slightly different when compared to *C. militaris* strains NBRC100741 (Schoch *et al.,* 2012) and JM0807 (Zhong *et al.*, 2010). Only one nucleotide (adenine, A) at position 93 of the ITS region of each studied strain was substituted by guanine (G) of NBRC100741 stain (Schoch *et al.,* 2012) (Fig. 5A). Furthermore, a nucleotide at position 136 in the 28S rRNA region of JM0807 strain was inserted by a thymine base (T) compared to all studied strains, as previously reported by Zhong *et al.* (2010) (Fig. 5B). In summary, all studied strains showed no genetic diversity; however, they exhibited a few nucleotide differences which might be caused by evolutionary effects such as nucleotide substitution and insertion from NBRC100741 and JM0807 strains (Ajawatanawong and Baldauf, 2013). Nucleotide substitutions and insertions can be correlated with the evolutionary distance (Park and Min, 2005) and provide information for phylogenetic reconstruction (Watanabe *et al.*, 2011) within fungal species.

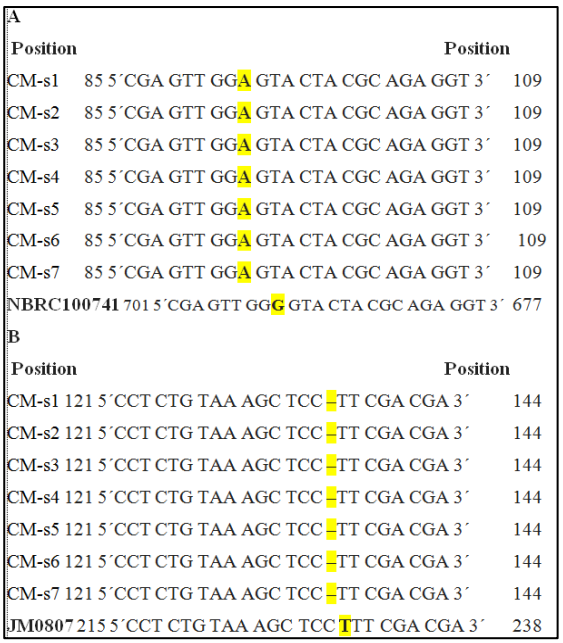

Fig. 5. Nucleotide mutation in C. militaris showing nucleotide substitution in ITS region (A) and nucleotide deletion in 28S rRNA region (B).

Note: the nucleotide highlighted with yellow color indicates nucleotide either substitution or addition. The hyphen highlighted with yellow color indicates nucleotide deletion.

Conclusions

Seven strains of *C. militaris* collected from different commercial farms in Thailand were investigated for morphological diversity using both macroscopic and microscopic methods. In the macroscopic studies, results concluded that most strains had high mycelial growth rate and abundant mycelial density with rough and semi-cottony mycelial texture, and yellowish colonies. Of these, CM-s4 had the lowest

growth rate; its mycelium was compact, formed of dense layers, and dark yellow on PDA. In the microscopic studies using a cross section technique, the stromal characteristics revealed that all strains were golden yellow at the edge with colorless hyphae. Conidial formation was studied using slide culture and SEM techniques. Results determined that most ascospores were globose and oval shaped; moreover, these germinated and produced long hyphae. At the ends of the hyphae, most conidia were formed as single globe heads but rarely as global groups in short chains. A few conidia were formed with an oval shape.

Genetic diversity among the seven strains was evaluated using nucleotide sequence analysis of ITS and 28S rRNA regions. Results concluded that all studied strains showed no genetic diversity; however, they had one nucleotide substitution in the ITS region and one nucleotide deletion in the 28S rRNA region. Further research is necessary to collect live specimens of the seven *C. militaris* strains to examine other molecular markers such as random amplification of polymorphic (RAPD), terminal restriction fragment (TRF) and amplified ribosomal DNA restriction analysis (ARDRA). Morphological characteristics can be further assessed using the shooting and slide culture techniques.

Acknowledgments

This study was financially supported by Naresuan University, Thailand and the Agricultural Research Development Agency (ARDA; Project number CRP5805020130). We are extremely grateful to both these organizations.

References

Ajawatanawong P, Baldauf SL. 2013. Evolution of protein indels in plants, animals and fungi. BMC Evolutionary Biology 13, 140.
https://doi.org/10.1186/1471-2148-13-140

Albini, M, Joseph E, Junier P. 2017. Fungal biogenic patina: optimization of an innovative conservation treatment for copper-based artefacts. PhD thesis. Université de Neuchâtel, Faculté des sciences 200.
http://doc.rero.ch/record/322673/files/00002593.pdf

Avtonomova AV, Krasnopolskaya LM, Shuktueva MI, Isakova EB, Bukhman VM. 2015. Assessment of Antitumor Effect of Submerged Culture of *Ophiocordyceps sinensis* and *Cordyceps militaris*. Antibiot Khimioter **60(7-8),** 14-17.

Brown AHS, Smith G. 1957. The genus *Paecilomyces bainier* and its perfect stage *Byssochlamys westling*. Transactions of the British Mycological Society **40(1),** 17-89.
https://doi.org/10.1016/s0007-1536(57)80066-7

Bunyard BA, Nicholson MS, Royse DJ. 1994. A systematic assessment of *Morchella* using RFLP analysis of the 28S ribosomal RNA gene. Mycologia **86(6),** 762-772.
https://doi.org/10.1080/00275514.1994.12026481

Chiu CP, Liu SC, Tang CH, Chan Y, El-Shazly M, Lee CL, Du YC, Wu TY, Chang FR, Wu YC. 2016. Anti-inflammatory Cerebrosides from Cultivated *Cordyceps militaris*. Agricultural and Food Chemistry **64(7),** 1540–154.
https://doi.org/10.1021/acs.jafc.5b0593

Dang HN, Wang CL, Lay HL. 2017. Effect of nutrition, vitamin, grains, and temperature on the myceliumgrowth and antioxidant capacity of *Cordyceps militaris* (strains AG-1and PSJ-1). Rediation Reseach and Applied Science **11,** 130-138.
https://doi.org/10.1016/j.jrras.2017.11.003

Guo LX, Hong YH, Zhou QZ, Zhu Q, Xu XM, Wang JH. 2017. Fungus-larva relation in the formation of *Cordyceps sinensis* as revealed by stable carbon isotope analysis. Scientific Reports **7(1),** 7789.
https://doi.org/10.1038/s41598-017-08198-1

Guo LX, Hong YH, Zhou QZ, Zhu Q, Xu XM, Wang JH. 2017. Fungus-larva relation in the formation of *Cordyceps sinensis* as revealed by stable carbon isotope analysis. Scientific Reports **7(1),** 7789.
https://doi.org/10.1038/s41598-017-08198-1

Kang N, Lee HH, Park I, Seo YS. 2017. Development of high cordycepin-producing *Cordyceps militaris* strains. Mycobiology **45(1),** 31-38.
http://doi.org/10.5941/MYCO.2017.45.1.31

Lam KY, Chan GK, Xin GZ, Xu H, Ku CF, Chen JP, Yao P, Lin HQ, Dong TT, Tsim KW. 2015. Authentication of *Cordyceps sinensis* by DNA Analyses: Comparison of ITS sequence analysis and RAPD-derived molecular markers. Molecules **20(12),** 22454–22462.
https://doi.org/10.3390/molecules201219861

Lee BJ, Lee MA, Kim YG, Lee KW, Choi YS, Lee BE, Song HY. 2013. Cultural characteristics of *Cordyceps militaris* strain 'Yedang 3' on various media and nutritional conditions. Mushroom Science and Production **11(3),** 124-130.
https://doi.org/10.14480/JM.2013.11.3.124

Li Y, Jiao L, Yao YJ. 2013. Non-concerted ITS evolution in fungi, as revealed from the important medicinal fungus *Ophiocordyceps sinensis*. Molecular Phylogenetics and Evolution **68,** 373-379.
https://doi.org/10.1016/j.ympev.2013.04.010

Lin LT, Lai YJ, Wu SC, Hsu WH, Tai CJ. 2018. Optimal conditions for cordycepin production in surface liquid-cultured *Cordyceps militaris* treated with porcine liver extracts for suppression of oral cancer. Journal of Food and Drug Analysis **26(1),** 135 -144.
https:/doi.org/10.1016/j.jfda.2016.11.021

Liu HJ, Hu HB, Chu C, Li Q, Li P. 2011. Morphological and microscopic identification studies of *Cordyceps* and its counterfeits. Acta Pharmaceutica Sinica B. **1(3),** 189-195.
https://doi.org/10.1016/j.apsb.2011.06.013

Liu JY, Feng CP, Li X, Chang MC, Meng JL, Xu LJ. 2016. Immunomodulatory and antioxidative activity of *Cordyceps militaris* polysaccharides in mice. International Journal of Biological Macromolecules **86,** 594–598.
https://doi.org/10.1016/j.ijbiomac.2016.02.009

Ma L, Zhang S, Du M. 2015. Cordycepin from *Cordyceps militaris* prevents hyperglycemia in alloxan-induced diabetic mice. Nutrition Research **35(5),** 431-439.
https://doi.org/10.1016/j.nutres.2015.04.011

Park YJ, Min BR. 2005. Sequence Analysis of the Internal Transcribed Spacer of Ribosomal DNA in the Genus *Rhizopus*. Mycobiology **33(2),** 109-112.
https://doi.org/10.4489/MYCO.2005.33.2.109

Petch T. 1936. *Cordyceps militaris* and *Isaria farinosa*. Transactions of the British Mycological Society **20(3–4),** 216-224.
https://doi.org/10.1016/S0007-1536(36)80014-X

Pettit RH. 1895. Studies in artificial cultures of entomogenous fungi. Bulletin (Cornell University. Agricultural Experiment Station) 97, 339-378.

Raethong N, Laoteng K, Vongsangnak W. 2018. Uncovering global metabolic response to cordycepin production in *Cordyceps militaris* through transcriptome and genome-scale network-driven analysis. Scientific Reports **8,** 9250.
https://doi.org/10.1038/s41598-018-27534-7

Schoch CL, Seifert KA, Huhndorf S, Robert V, Spouge JL, Levesque CA, Chen W. 2012. Fungal Barcoding Consortium; Fungal Barcoding Consortium Author List. Nuclear ribosomal internal transcribed spacer (ITS) region as a universal DNA barcode marker for Fungi. Microbiology **109(16),** 6241-6246.
https://doi.org/10.1073/pnas.1117018109

Shrestha B, Han SK, Yoon KS, Sung JM. 2005. Morphological Characteristics of Conidiogenesis in *Cordyceps militaris*. Mycobiology 33(2), 69-76.
https://doi.org/10.4489/MYCO.2005.33.2.069

Song J, Wang Y, Teng M, Zhang S, Yin M. 2016. *Cordyceps militaris* induces tumor cell death via the *caspased*ependent mitochondrial pathway in HepG2 and MCF7 cells. Molecular Medicine Reports **13(6),** 5132-5140.
https://doi.org/10.3892/mmr.2016.5175

Sung GH, Shrestha B, Han SK, Sung JM. 2011. Growth and Cultural Characteristics of *Ophiocordyceps longissima* Collected in Korea. Mycobiology **39(2),** 85-91.
https://doi.org/10.4489/MYCO.2011.39.2.085

Ta H. 1999. BioEdit: a user-friendly biological sequence alignment editor and analysis program for Windows 95/98/NT. Nucleic Acids Symposium Series **41,** 95-98.

Tapingkae T. 2012. *Cordyceps* mushroom cultivation. Bangkok: Two Four Printing, 15-62. (Thai article)

Tatani K, Hiratochi M, Kikuchi N, Kuramochi Y, Watanabe S, Yamauchi Y. 2016. Identification of adenine and benzimidazole nucleosides as potent human concentrative nucleoside transporter 2 inhibitors: potential treatment for hyperuricemia and gout. Journal of Medicinal Chemistry **59(8),** 3719-3731. https://doi.org/10.1021/acs.jmedchem.5b01884

Tianzhu Z, Shihai Y, and Juan D. 2015. The effects of cordycepin on ovalbumin-induced allergic inflammation by strengthening treg response and suppressing Th17 responses in ovalbumin-sensitized mice. Inflammation **38(3),** 1036-1043. https://doi.org/10.1007/s10753-014-0068-y

Tulasne LR, Tulasne C. 1865. Selecta *Fungorum Carpologia*. vol. 3. (English translation). Clarendon Press, Oxford.

Watanabe M, Yonezawa T, Lee K, Kumagai S, Sugita-Konishi Y, Goto K, Hara-Kudo Y. 2011. Molecular phylogeny of the higher and lower taxonomy of the *Fusarium* genus and differences in the evolutionary histories of multiple genes. BMC Evolutionary Biology **11** 322. https://doi.org/10.1186/1471-2148-11-322

Wen TC, Long FY, Kang C, Wang F, Zeng W. 2017. Effects of additives and bioreactors on cordycepin production from *Cordyceps militaris* in liquid static culture. Mycosphere **8(7)**, 886-898.

White T, Burns J, Lee S, Taylor J. 1990. Amplification and direct sequencing of fungal ribosoma lRNA genes for phylogenetics. In Innis, M. A. D. H. Gelfand, J. J. Sinsky, and T. J. White. (Eds.), PCR protocols: a guide to methods and applications. Academic Press, San Diego, California 482

Yong T, Zhang M, Chen D, Shuai O, Chen S, Su J. 2016. Actions of water extract from *Cordyceps militaris* in hyperuricemic mice induced by potassium oxonate combined with hypoxanthine.

Zhang P, Huang C, Fu C, Tian Y, Hu Y, Wang B. 2015. Cordycepin (3′-deoxyadenosine) suppressed HMGA2, Twist1 and ZEB1-dependent melanoma invasion and metastasis by targeting miR-33b. Oncotarget **6(12),** 9834-9853. https://doi.org/10.18632/oncotarget.3383

Zhang P, Huang C, Fu C, Tian Y, Hu Y, Wang B. 2015. Cordycepin (3′-deoxyadenosine) suppressed HMGA2, Twist1 and ZEB1-dependent melanoma invasion and metastasis by targeting miR-33b. Oncotarget **6,** 9834-9853. https://doi:10.18632/ oncotarget.3383.

Zhong X, Peng Q, Qi L, Lei W, Liu X. 2010. rDNA-targeted PCR primers and FISH probe in the detection of *Ophiocordyceps sinensis* hyphae and conidia. Microbiological Methods **83(2)**, 188-193. https://doi.org/10.1016/j.mimet.2010.08.020.